ORIGINAL ARTICLE



Quantitative trait loci for rolled leaf in a wheat EMS mutant from Jagger

Ruolin Bian¹ · Na Liu^{1,2} · Yuzhou Xu¹ · Zhenqi Su^{1,3} · Lingling Chai^{1,3} · Amy Bernardo⁴ · Paul St. Amand⁴ · Allan Fritz¹ · Guorong Zhang¹ · Jessica Rupp⁵ · Eduard Akhunov⁵ · Katherine W. Jordan⁴ · Guihua Bai^{1,4}

Received: 17 August 2022 / Accepted: 26 November 2022 / Published online: 13 March 2023
This is a U.S. Government work and not under copyright protection in the US; foreign copyright protection may apply 2023

Abstract

Key message Two QTLs with major effects on rolled leaf trait were consistently detected on chromosomes 1A (QRl. hwwg-1AS) and 5A (QRl.hwwg-5AL) in the field experiments.

Abstract Rolled leaf (RL) is a morphological strategy to protect plants from dehydration under stressed field conditions. Identification of quantitative trait loci (QTLs) underlining RL is essential to breed drought-tolerant wheat cultivars. A mapping population of 154 recombinant inbred lines was developed from the cross between JagMut1095, a mutant of Jagger, and Jagger to identify quantitative trait loci (QTLs) for the RL trait. A linkage map of 3106 cM was constructed with 1003 unique SNPs from 21 wheat chromosomes. Two consistent QTLs were identified for RL on chromosomes 1A (*QRl.hwwg-1AS*) and 5A (*QRl.hwwg-5AL*) in all field experiments. *QRl.hwwg-1AS* explained 24–56% of the phenotypic variation and *QRl.hwwg-5AL* explained up to 20% of the phenotypic variation. The combined percent phenotypic variation associated with the two QTLs was up to 61%. Analyses of phenotypic and genotypic data of recombinants generated from heterogeneous inbred families of JagMut1095×Jagger delimited *QRl.hwwg-1AS* to a 6.04 Mb physical interval. This work lays solid foundation for further fine mapping and map-based cloning of *QRl.hwwg-1AS*.

Introduction

Drought is one of the most harmful environmental stresses for crops in most rain-fed areas worldwide. Drought not only reduces crop yield, but also reduces the availability of land for agriculture. Plant phenology allows the crop demand to synchronize with environmental resource availability and escape from seasonal abiotic stresses (Bogard et al. 2021). Breeding for cultivars with increased tolerance to drought

Communicated by Xianchun Xia.

- ☐ Guihua Bai guihua.bai@usda.gov
- Department of Agronomy, Kansas State University, Manhattan, KS 66506, USA
- Henan Agricultural University, Zhengzhou 450002, Henan Province, China
- China Agricultural University, Beijing 100083, China
- ⁴ USDA-ARS, Hard Winter Wheat Genetics Research Unit, Manhattan, KS 66506, USA
- Department of Plant Pathology, Kansas State University, Manhattan, KS 66506, USA

and heat has been the most effective strategy to reduce the negative impact of drought on crop production (Verma et al. 2020). However, the global climate change has been projected to increase air temperature and raise water demand of rain-fed and irrigated crops, which creates a major challenge for breeders to improve the adaptation to increased drought and heat stress during flowering and grain filling of winter and spring crops such as wheat and barley (Gouache et al. 2012; Sommer et al. 2013).

Drought-tolerant plants use biochemical, physiological, or morphological strategies to cope with drought stress (Turner and Begg 1981; Kadioglu and Terzi 2007). Rolled leaf (RL) in plants, including leaf folding and paraheliotropism, is one of the morphological strategies for dehydration avoidance mechanism to protect plant leaves from photodamage under drought conditions in field (Corlett et al. 1994). RL under drought stress reduces leaf area under solar radiation or lowers transpiration rates through the creation of a microclimate near the leaf surface (Oppenheimer 1960; Turner and Begg 1981). Under drought stress, the closed stomata reduce transpiration, CO₂ uptake, and photosynthetic activity, which generates an imbalance between PSII activity and the Calvin cycle to increase the excitation energy on PSII leading to

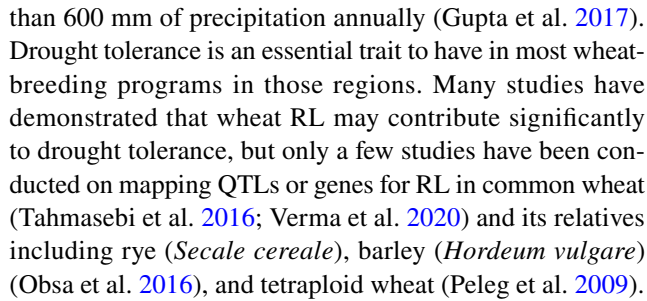


subsequent photodamage (Baker and Rosenqvist 2004). RL, however, helps a plant maintain leaf hydration, but keeps stomata open to prevent losses of photosynthetic pigments and sustain the activities of PSII and Rubisco (Saglam et al. 2014). Additionally, RL is reversible, which provides the flexibility to reduce the radiation load on the canopy only when necessary. All the benefits from RL under drought stress make RL an important target trait for drought tolerance breeding in several crops including wheat (*Triticum aestivum* L.) (Myşków et al. 2018).

In plants, several factors including water deficit, high air temperature, or high radiation from sunlight can cause RL. Depending on the populations, genetic variation in RL trait may be generated by a single gene with a major effect (Singh and Mackill 2008) or multiple genes with minor effects (Price et al. 1997). In rice, more than 70 genes or quantitative trait loci (QTLs) have been identified for RL and at least 17 mutants have been characterized for adaxially or abaxially RL (Liu et al. 2016; Qiang et al. 2016). Remarkably, at least 18 cloned genes for RL in rice are related to bulliform cells, a group of thin-walled and highly vacuolated large cells between the vascular bundles on the adaxial epidermis of a rice leaf blade (Gao et al. 2019). For example, the rice outermost cell-specific gene 5 (Roc5), a member of the class IV HD-Zip genes, controls the number and size of bulliform cells, while the overexpression of Roc5 caused adaxially RL (Zou et al. 2011). Semi-rolled leaf1 (SRL1) is another rice RL gene encoding a putative glycosylphosphatidylinositolanchored protein and modulates RL by regulating the formation of bulliform cells at the adaxial cell layers (Xiang et al. 2012). A zinc finger homeodomain class homeobox transcription factor (OsZHD1) has also been reported to increase the number and the abnormal arrangement of the bulliform cells to cause abaxially RL (Xu et al. 2014).

In maize, RL is selected by breeders to enhance plant density tolerance by reducing the mass shading factors (Gao et al. 2019). To date, five maize RL mutants have been reported including *leafbladeless1* (*Lbl1*) and *rolled leaf1* (*rld1*) (Timmermans et al. 1998; Juarez et al. 2004). The *Lbl1* mutant has abaxialized leaves due to a complete loss of adaxial cell types. *Rld1* encodes a class III homeodomain-leucine zipper (HD-ZIP III) protein that is required for specifying adaxial cell fate and controlling upward curling of leaf blades (Juarez et al. 2004). Beside bulliform cells (number and size) and leaf polarity (Adaxial/Abaxial), genes for RL may also contribute to development of sclerenchymatous cells and cuticle, but the physiological and molecular mechanisms underlying these genes remain unknown (Xu et al. 2018).

Wheat is a staple food crop, accounting for 20% of calories and proteins consumed by the world's population (Shiferaw et al. 2013). In developing countries, almost 50% of wheat (50 million ha) is sown under rain-fed areas with less



Single-nucleotide polymorphism (SNP) markers generated by genotyping-by-sequencing (GBS) have been frequently used in QTL mapping. Previously, we developed a RIL population from a cross between Jagger and an ethyl methanesulfonate (EMS)-induced mutant (JagMut1095) of Jagger. The objectives of this study were to identify QTLs controlling the RL trait using the RIL population of JagMut1095×Jagger and provide the foundation for map-based cloning and functional characterization of RL genes in the mutant.

Materials and methods

Plant materials

Jagger (PI 593688) is a hard winter wheat cultivar from Kansas and does not show visible RL in the field. JagMut1095 is a mutant that was selected from the mutant population derived by EMS mutagenesis of Jagger as described by Rawat et al. (2019) and showed significant RL in both the field and greenhouse conditions spontaneously. An M_5 mutant plant (JagMut1095) derived by single seed descent in the greenhouse was crossed to Jagger and a population of 154 RILs developed from the cross of JagMut1095×Jagger was used for QTL analysis.

Phenotyping the rolled leaf trait in the field

The RL trait was scored in five field experiments conducted in three Kansas locations (Ashland Bottoms Research Farm and Rocky Ford Research Station, Manhattan, KS and Agricultural Research Center at Hays, KS) for two wheat-growing seasons (2019–2020 and 2020–2021) with the loss of the experiment at Hays in the 2020–2021 season due to severe hail damage. The five experiments were designated as combinations of years and locations of the experiments conducted (2020-Ashland, 2020-Rocky-Ford, 2020-Hays, 2021-Ashland and 2021-Rocky-Ford). The F₈ RIL population was planted with two replications and the parents with five replications using a randomized complete block design (RCBD) in each experiment. One gram of seeds per line was sowed in a 1-m-long single-row plot. RL was visually scored on a 1 (no rolled leaf) to



5 (complete rolled leaf) scale at noon during sunny days after flowering (Supplemental Figure S1a).

Genotyping the parents and RIL population

Leaf tissues were collected at the three-leaf stage from a single plant of each F₅ RIL and parents into 96-deepwell plates, dried in a freeze dryer (ThermoFisher, Waltham, MA) for 48 h, and then ground into fine powder at 30 cycles/sec for 3 min in a GenoGrinder 2010 tissue grinder (SPEX SamplePrep, NJ, USA). DNA was isolated using a modified cetyltrimethyl ammonium bromide (CTAB) method (Bai et al. 1999). DNA concentration was estimated using a Quant-iTTM PicoGreen® dsDNA Assay kit (ThermoFisher Scientific, Waltham, MA) in a FLUOstar Omega microplate reader (BMG LABTECH, German), and normalized to 20 ng/µL for GBS library construction (Poland and Rife 2012). In brief, normalized genomic DNA was double-digested using restriction enzymes PstI and MspI (New England Biolabs Inc., Ipswich, MA) and ligated to a set of barcode adapters using T4 ligase (New England Biolabs Inc). The GBS library was sizeselected for 200-300 bp fragments in an E-gel system (ThermoFisher Scientific). The selected polymerase chain reaction (PCR) fragments were purified with the GenCatch PCR purification kit (Epoch Life Science Inc., Sugar Land, TX), and quantified with the Qubit dsDNA HS assay kit (ThermoFisher Scientific) before sequencing using PI v3 chips and Hi-Q sequencing kits (ThermoFisher Scientific) in an Ion Torrent Proton sequencer (Life Technologies, Carlsbad, CA). The raw sequence reads were assigned to each sample based on attached barcodes, then trimmed to 64 bp DNA sequences including the 5' restriction site. SNPs were detected using a reference-based pipeline in TASSEL 5.0 (Bradbury et al. 2007) using the IWGSC Ref-Seq v2.1 genome (IWGSC 2018) to assign the physical positions for each SNP. Exome-capture data were obtained for JagMut1095 and Jagger using an assay described previously (Jordan et al. 2015). The quality of raw sequencing reads was assessed using NGSQC toolkit v.2.3.3 (Patel and Jain 2012). The sequence reads were aligned to the IWGSC wheat reference genome RefSeq v.1.1 (IWGSC 2018) using HISAT2 (Kim et al. 2015) retaining only uniquely mapped reads. The resulting alignments were processed using Samtools (Li et al. 2009) and run through the GATK pipeline (McKenna et al. 2010) using Haplotype Caller to generate a variant call file including variants for Jagger and the Jagger mutant. Additional SNPs in the identified QTL intervals were used to increase marker density. The position of each exome-capture SNP on the IWGSC wheat reference genome RefSeq v.2.1 (IWGSC 2018) was decided by blasting the flanking sequence of each SNP.

KASP marker development and validation

In the major QTL intervals for RL, primers for kompetitive allele-specific PCR (KASP) were designed based on the SNP sequences generated from both GBS and exome capture using Primer3web version 4.1.0 (http://primer3.wi.mit.edu/) (Untergasser et al. 2012). The PCR allele Competitive extension (PACE) assays were performed to screen KASP primers in parents and the RIL population. Markers segregating at expected ratios in the RIL population were used to refine the genetic map in the QTL regions. Each PACE assay consists of 1.94 µL of 2X PACETM reaction mix (3CR Bioscienc, Harlow, England, UK), 0.06 µL of primer assay mix, and 2 μL of 20 ng/μL DNA. The PCR initially started at 94 °C for 15 min, followed by 10 cycles at 94 °C for 20 s, 65 °C for 1 min with -0.8 °C in each subsequent cycle to 57 °C, then by 30 cycles of 94 °C for 20 s, and 57 °C for 1 min.

Linkage map construction and QTL analysis

The linkage map was constructed using QTL IciMapping v4.1 (Wang et al. 2009; Meng et al. 2015). Individual linkage groups of GBS-SNPs were anchored to 21 corresponding chromosomes based on IWGSC RefSeq v2.1 (IWGSC 2018). The Kosambi mapping function was used to convert recombination frequency to genetic distance in the linkage map (Kosambi 1943). The TwoOpt algorithm was used to order the SNPs in each linkage group, and SARF (Sum of adjacent recombination frequencies) module was used for fine-tuning of the marker order in each linkage group.

QTL analysis was performed using the composite interval mapping (CIM) module in QTL Cartographer v2.5 (Wang et al. 2007) with a walking speed of 1.0 cM. The averaged RL score over two replications in each environment and the adjusted mean best linear unbiased estimators (BLUE) were calculated for five environments and were included in QTL analysis. The significant QTLs were claimed at the LOD threshold of 4.10 for RL and at 4.0 for HD derived by 1000-time permutations of the BLUE values using QTL Cartographer v2.5 (Doerge and Churchill 1996; Wang et al. 2007). QTL names were designated using standard QTL nomenclature starting with Q representing QTL, followed by the abbreviations of the trait name (RL for rolled leaf) and the institute name (Hwwg for Hard Winter Wheat Genetic Research Unit), then by chromosome (or arm) location where the OTL is located after a dash line. OTLs that mapped at the same or overlapping locations were considered as the same QTLs and a QTL that was significant in two or more experiments was considered as a stable QTL.



Results

Rolled leaf scores in parents and RILs

The BLUE of RL score across all five environments was 4.77 for JagMut1095, and 1.05 for Jagger. The differences in RL were significant (P < 0.0001) between the parents and among the RILs of JagMut1095×Jagger across the five experiments. The frequency of RL scores for the RIL population did not follow a normal distribution (Fig. 1; Shapiro–Wilk test P < 0.0001). The mean RL score over the five experiments was 2.88, ranging from 1.07 to

5.00 and the coefficient of variation (CV) ranged from 40.22 to 53.05%. High positive correlations (0.66–0.84; P < 0.001) were observed for RL scores between the five experiments (Table 1). The broad sense heritability for RL was high, ranging from 0.73 in 2020-RockyFord to 0.92 in 2020-Hays. The effects of genotypes, environments, and genotype-by-environment interactions on RL scores were highly significant (P < 0.0001) (Table S1). The RL significantly correlated with HD (r = 0.41; P < 0.001), but the correlations between RL and PH were not significant across the five environments (P > 0.05).

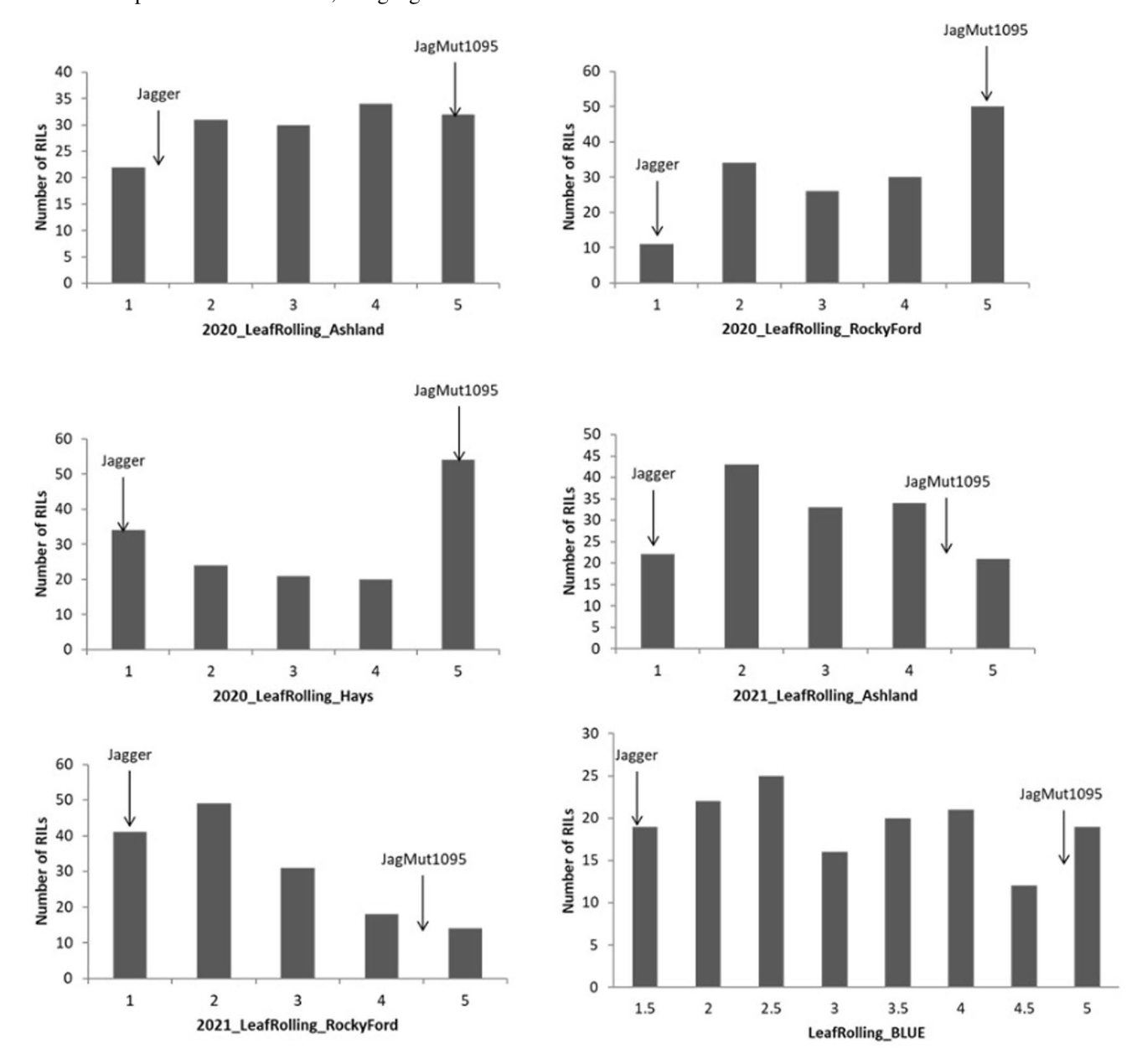


Fig. 1 Frequency distribution of rolled leaf scores for the recombinant inbred population of JagMut1095×Jagger in five experiments and BLUE



Table 1 The correlation coefficients of rolled leaf scores among the five environments

	2020-Hays	2021-Ashland	2021-Rockyford	2020-Ashland
2021-Ashland	0.836***			
2021-Rockyford	0.704***	0.834***		
2020-Ashland	0.813***	0.799***	0.661***	
2020-Rockyford	0.799***	0.724***	0.692***	0.710***

^{***}Refers to the highly significant correlation at P < 0.001

SNP genotyping and linkage map construction

Sequencing the GBS libraries of 154 RILs and their parents identified 66,081 SNPs, with 23,206 SNPs in the A genome, 29,535 SNPs in the B genome, and 13,340 SNPs in the D genome. Chromosome 1B had the most markers (5306), and chromosome 4D had the least (1450). After removal of SNPs with > 20% missing data, > 10% heterozygotes or < 20% minor allele frequency, 3703 high-quality SNPs were used for construction of a genetic map. After binning the SNPs that mapped at the same location, only 1003 unique SNPs were mapped to 22 linkage groups corresponding to the 21 chromosomes with a total map length of 3106 cM and a marker density of 3.1 cM per marker (Fig. S2).

QTL analysis and KASP marker development

QTL analysis using CIM module identified two stable QTLs on chromosomes 1A and 5A, designated as QRl.hwwg-1AS and QRl.hwwg-5AL. These two QTLs were consistently significant in multiple environments with the both RL alleles derived from JagMut1095 (Table 2, Fig. 2). QRl.hwwg-1AS was mapped to the distal end of chromosome arm 1AS between Exon1A-35 (3,442,958 bp) and *Exon1A-45* (11,012,144 bp), and showed the largest effect that explained 24% to 56% of the phenotypic variation. QRl.hwwg-5AL was mapped near the centromere of 5AL between 228,517,222 and 456,003,747 bp in one environment and between 441,373,760 and 491,620,424 bp in other four environments and for BLUE, which explained up to 20% of the phenotypic variation (Table 2, Fig. 2a). As RL and HD showed a significant positive correlation in the field experiments (0.41; P < 0.001), QTL analysis on HD was conducted to check possible overlapped QTLs between RL and HD in the two RL QTL intervals (Table 2). As the result, one HD QTL was detected on chromosome 1A in the 2020-Ashland experiment and BLUE (LOD = 5.11-6.98) with the later heading allele from JagMut1095. This QTL overlapped with QRl.hwwg-1AS for RL. In addition, four other HD QTLs were detected on chromosomes 2B, 5B, 5D, and 7B with all the later heading alleles from JagMut1095 except 5D QTL from Jagger and they did not overlap with any RL QTL. Among these HD QTLs, the 2B QTL (64,462,647, and 75,415,490 bp) explained the largest phenotypic variation (PVE).

To increase SNP density in the QRl.hwwg-1AS region, additional KASP markers were designed using the flanking sequence of the SNPs identified within or close to the QTL region from exome-capture assays. Among the 47 pairs of primers screened, 17 were polymorphic between the parents. Among these polymorphic markers, eight clearly segregated among the RILs (Supplemental Table S2, Fig. 3), therefore were added to the chromosome 1A linkage map for QTL analysis. The physical locations of the eight KASP markers are mapped from 3,381,332 to 12,956,070 bp based on the IWGSC RefSeq v2.1 genome. After removal of markers that were mapped to the same position, five markers, Exon1A-17, Exon1A-25, Exon1A-28, Exon1A-35, and Exon1A-45, remained in the genetic map. The order of these markers in the genetic map was consistent with their physical positions in the IWGSC RefSeq v2.1 genome (Fig. 2b, c).

Candidate interval of QRI.hwwg-1AS

To further narrow down the candidate interval of QRl. hwwg-1AS, one F₄ heterogeneous inbred family (HIF) was identified from JagMut1095 × Jagger population and used to develop recombinants within the QTL region. One pair of near-isogenic lines (NILs), L73-8-3 and L73-8-4, with a recombination within the QTL region was identified and showed significant contrast in the RL levels (5 and 2, respectively) in all the three replications in year 2022-RockyFord (Fig. 2b, c). This moved the right border of the candidate QTL interval to left side of Exon1A-25 (9,482,836 bp) based on IWGSC RefSeq v2.1. Two RILs (RIL-74 and RIL-76) each showed a recombination at the right site of the marker Exon1A-35 (Fig. 2c) and phenotypic data of the two RILs defined the Exon1A-35 as the left flanking of QRl.hwwg-1AS. Therefore, these data delimited QRl.hwwg-1AS to a 6 Mb interval between Exon1A-35 (3,442,958 Mb) and Exon1A-25 (9,482,836 bp).

Discussion

RL has been considered as an important morphological trait involved in drought stress response and has been shown to have either monogenic (Singh and Mackill 2008) or polygenic inheritance (Price et al. 1997). Although studies on



 $\textbf{Table 2} \ \ \text{The parameters generated from composite interval mapping (CIM) using rolled leaf (RL) scores collected from the RIL population of \\ JagMut1095 \times Jagger evaluated in five field experiments$

QTL name	Environments	Chromosome	Position (cM)	Peak interval (cM)	LOD	Add	R^2	Flanking markers	Physical interval in CS RefSeq (v2.1)
QRl.hwwg-1AS	2020-Ashland- RL	1A	3.71	2.2–6.7	13.51	0.84	0.36	Exon1A-35- Exon1A-45	3,442,958– 11,012,144
	2020-Rocky- Ford-RL	1A	2.71	0-5.9	15.92	0.76	0.30	Exon1A-35- Exon1A-45	3,442,958– 11,012,144
	2020-Hays-RL	1A	3.71	2.8–5.8	33.90	1.24	0.56	Exon1A-35- Exon1A-45	3,442,958– 11,012,144
	2021-Rocky- Ford-RL	1A	2.71	0–5.8	14.57	0.60	0.24	Exon1A-35- Exon1A-45	3,442,958– 11,012,144
	2021-Ashland- RL	1A	3.71	2.3–6	21.45	0.74	0.29	Exon1A-35- Exon1A-45	3,442,958– 11,012,144
	BLUE-RL	1A	2.71	2.3–6	27.29	0.80	0.44	Exon1A-35- Exon1A-45	3,442,958– 11,012,144
QRl.hwwg-5AL	2020-Rocky- Ford-RL	5A	65.01	62.3–68.5	5.93	0.31	0.09	S5A_441373760- S5A_491620424	441,373,760– 491,620,424
	2020-Ashland- RL	5A	64.11	62.3–65.8	5.34	0.40	0.08	S5A_441373760- S5A_491620424	441,373,760– 491,620,424
	2020-Hays-RL	5A	65.01	63.3–68	4.81	0.34	0.05	S5A_441373760- S5A_491620424	441,373,760– 491,620,424
	2021-Rocky- Ford-RL	5A	41.81	40.8–43.8	11.65	0.56	0.20	S5A_228517222- S5A_456003747	228,517,222– 456,003,747
	2021-Ashland- RL	5A	64.11	62.3–65.5	11.86	0.51	0.15	S5A_441373760- S5A_491620424	441,373,760– 491,620,424
	BLUE-RL	5A	64.11	62.9–65.3	10.40	0.37	0.11	S5A_441373760- S5A_491620424	441,373,760– 491,620,424
QHd.hwwg-1AS	2020-Rocky- Ford-HD	1A	1.01	0–2.7	3.92	0.73	0.06	Exon1A-35- Exon1A-45	3,442,958– 11,012,144
	2020-Ashland- HD	1A	5.71	0–14	6.98			Exon1A-35- Exon1A-45	3,442,958– 11,012,144
	BLUE-HD	1A	3.71	2–8.9	5.11			Exon1A-35- Exon1A-45	3,442,958– 11,012,144
QHd.hwwg-2BS	2020-Rocky- Ford-HD	2B	125.81	125.7–127.5	11.49	1.40	0.21	S2B_64462647- S2B_75415490	64,462,647– 75,415,490
	2021-Rocky- Ford-HD	2B	126.31	125.8–128.1	7.71	1.23	0.14	S2B_64462647- S2B_75415490	64,462,647– 75,415,490
	2021-Ashland- HD	2B	126.31	125.8–127.9	10.02	1.04	0.20	S2B_64462647- S2B_75415490	64,462,647– 75,415,490
	BLUE-HD	2B	126.31	125.7–127.4	11.41	1.09	0.20	S2B_64462647- S2B_75415490	64,462,647– 75,415,490
QHd.hwwg-5BL	2020-Rocky- Ford-HD	5B	126.21	125.2–129.7	3.98	0.73	0.05	S5B_696551110- S5B_702517659	696,551,110– 702,517,659
	2021-Rocky- Ford-HD	5B	126.21	125.2–128	4.06	0.67	0.04	S5B_696551110- S5B_702517659	696,551,110– 702,517,659
	2020-Ashland- HD	5B	129.71	128.4–130.1	4.38	0.45	0.03	S5B_696551110- S5B_702172618	696,551,110– 702,172,618
	BLUE-HD	5B	126.21	122.6–128.7	5.25	0.64	0.07	S5B_697588246- S5B_702517659	697,588,246– 702,517,659
QHd.hwwg- 5DL	2020-Rocky- Ford-HD	5D	191.91	164.8–205.9	3.73	-0.80	0.05	S5D_510666142- S5D_444079953	444,079,953– 510,666,142
	2021-Rocky- Ford-HD	5D	182.91	169.7–196.2	5.70	-1.11	0.11	S5D_510666142- S5D_444079953	444,079,953– 510,666,142
	BLUE-HD	5D	181.91	180.6–183.3	7.39	-0.47	0.06	S5D_510666142- S5D_444079953	444,079,953– 510,666,142



Table 2 (continued)

QTL name	Environments	Chromosome	Position (cM)	Peak interval (cM)	LOD	Add	R^2	Flanking markers	Physical interval in CS RefSeq (v2.1)
QHd.hwwg-7BS	2020-Rocky- Ford-HD	7B	119.61	118.8–123.3	5.29	0.86	0.09	S7B_194609276- S7B_73904769	73,904,769– 194,609,276
	2021-Rocky- Ford-HD	7B	118.61	116–122.6	5.95	1.03	0.11	S7B_194609276- S7B_73904769	73,904,769– 194,609,276
	2021-Ashland- HD	7B	118.61	113–120.7	5.16	0.73	0.10	S7B_194609276- S7B_106813195	106,813,195– 194,609,276
	BLUE-HD	7B	120.61	116.2–123.3	5.06	0.69	0.09	S7B_194609276- S7B_73904769	73,904,769– 194,609,276

a LOD = log likelihood ratios

RL have been reported in different crop species (Xu et al. 2018; Gao et al. 2019; Myşków et al. 2018), only a few studies on QTL mapping for RL have been conducted in wheat. Verma et al. (2020) reported 12 QTLs for RL on wheat chromosomes 1B, 2A, 2B, 2D, 3A, 4A, 4B, 5D, and 6B (Verma et al. 2020); and Peleg et al. (2009) found 14 RL QTLs on chromosomes 1A, 2A, 2B (3), 3B, 4B, 5A, 5B, 6A, 6B, 7A, and 7B (2) of tetraploid wheat (T. turgidum ssp. Dicoccoides) (Peleg et al. 2009). The 1A QTL in tetraploid wheat was mapped near Xgwm691 between 23.3 and 56.5 cM. The physical location of Xgwm691 was unavailable, but the SSR marker *Xcfa2158a* at 21.7 Mb was located 7.6 cM distal to Xgwm691. Therefore, Xgwm691 is likely located between 21.7 Mb and centromere on 1AS. However, QRl.hwwg-1AS in the current study was mapped to the interval between 3.4 and 9.5 Mb in the distal end of 1AS, thus is far from Xgwm691, suggesting that QRl.hwwg-*1AS* identified in this study is most likely a new QTL for RL. QRl.hwwg-5AL was the second QTL consistently detected in different experiments in this study. Previously, one QTL for RL was mapped near Xgwm156 between 21.0 and 79.6 cM on 5AL of a tetraploid wheat (Peleg et al. 2009). Xgwm156 is located at 450.4 Mb in IWGSC RefSeq v2.1 (IWGSC 2018), which is within the *QRl.hwwg-5AL* interval (441.4) and 491.6 Mb). Therefore, it is possible that QRl.hwwg-5AL is the same QTL as the one reported by Peleg et al. (2009).

As *QRl.hwwg-1AS* explained the largest portion of the phenotypic variation, it was chosen for initial fine mapping. Phenotypic and genotypic analyses of RILs and the RILderived HIFs delimited the *QRl.hwwg-1AS* to a 6.04 Mb interval between the markers *Exon1A-35* (3,442,958 bp) and *Exon1A-25* (9,482,836 bp). Within this interval, 115 high confidence genes were annotated in Chinese Spring reference genome (IWGSC 2018), including *TraesCS1A03G0023500* and *TraesCS1A03G0027900* that are orthologs of cloned RL

genes in rice. TraesCS1A03G0023500 was annotated as a 20G-Fe (II) oxygenase family protein, a gene homolog of RL14 cloned in rice (Fang et al. 2012). RL14 was found to modulate rice RL by affecting secondary cell wall formation and inducing shrinkage and abnormal shape of bulliform cells. TraesCS1A03G0027900 was annotated as a cellulose synthase-like protein, and its ortholog NRL1 in rice encoded a cellulose synthase-like protein (OsCslD4) that induces a reduced leaf width and semi-rolled leaf by modulating the development of the vascular tissue and the cell wall biosynthesis (Hu et al. 2010). The current QRl. hwwg-1AS interval including 115 annotated genes remains too large for determining the causal candidate gene for the QTL and further fine mapping is needed to clone the gene. However, since the homologs of *TraesCS1A03G0023500* and TraesCS1A03G0027900 condition RL trait in rice, functional characterization of the two wheat genes may facilitate understanding of mechanisms of leaf rolling in wheat.

Reports on the effects of RL on drought tolerance remain controversial to date. Many studies demonstrated that RL reduced the leaf area under solar radiation or reduced the transpiration rates through the creation of a microclimate near the leaf surfaces, therefore benefited plants under drought stress (Turner and Begg 1981; Oppenheimer 1960). RL was reported to reduce the leaf surface area by 41-65% in wheat (Clarke 1986) and Ctenanthe setosa (Turgut and Kadioglu 1998). In rice, RL lost only 18% of initial fresh weight as compared to 38% loss in unrolled leaves after three hours dehydration (Singh and Singh 2000). However, some other studies suggested that RL may not be a morphological trait for drought tolerance because RL reduced the effective leaf area for light interception and increased the diffusive resistance to CO₂ to reduce photosynthesis efficiency (Hsiao et al. 1984). Saneoka and Waichi (1996) reported that the degree of RL in drought tolerant cultivars was lower than drought susceptible cultivars



b PVE=the phenotypic variation explained by a QTL

c ADD = additive effect in which a positive value indicates increased RL level contributed by JagMut1095

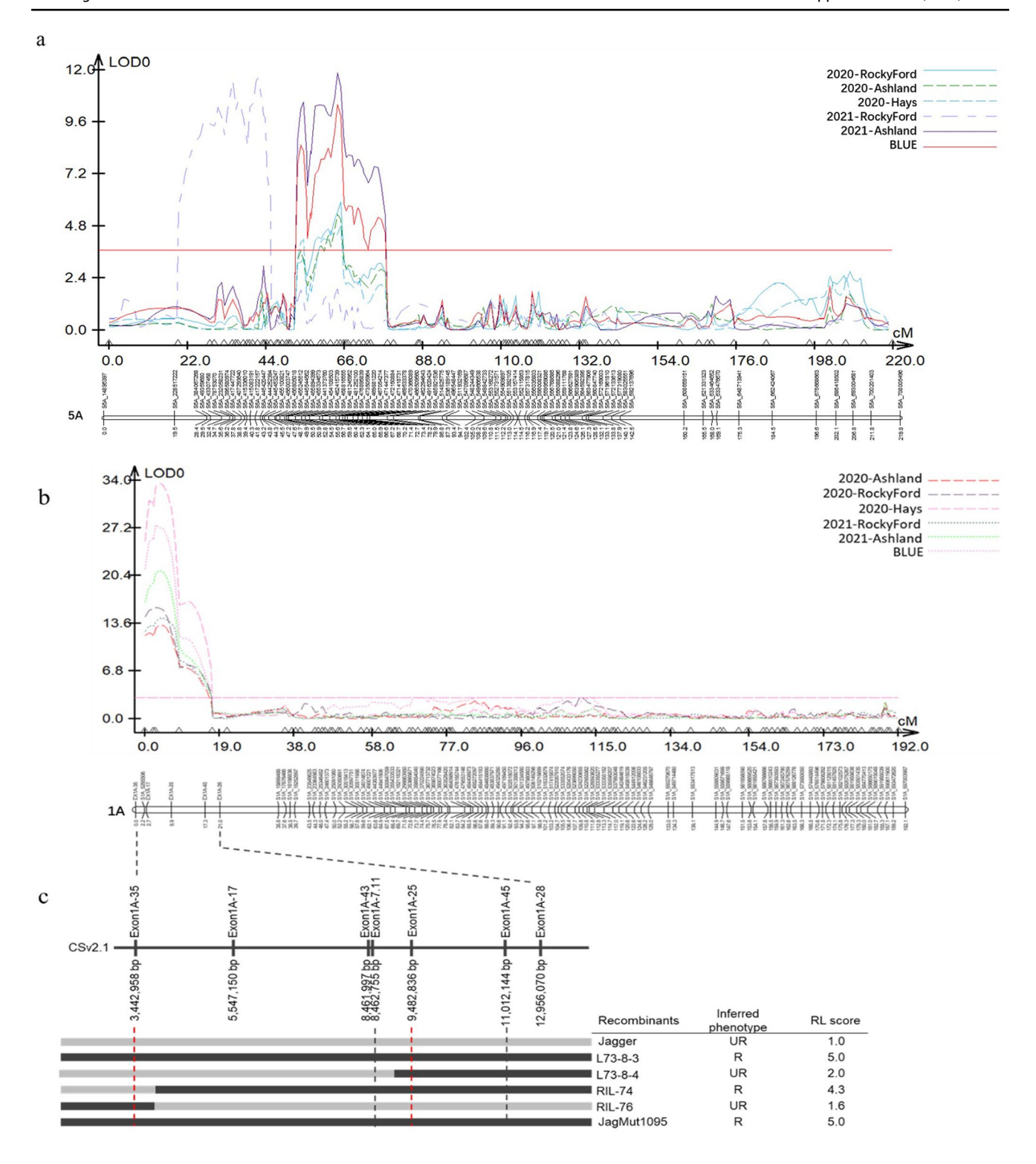


Fig. 2 Genetic maps of 5A and 1A and the map locations of *QRl. hwwg-5AL* and *QRl.hwwg-1AS*. **a** A genetic map of 5A showing *QRl.hwwg-5AL* locations detected in the five field experiments; **b** a genetic map of 1A showing *QRl.hwwg-1AS* locations detected in the five field experiments; **c** a physical map of *QRl.hwwg-1AS* showing newly identified flanking marker positions (red dash lines). Rectan-

gular bars under the physical map represent recombinant lines with a recombination in the QTL region with black bar for JagMut1095 genotype and gray bar for Jagger genotype. The table on the right list the recombinant line name and their phenotypic data (colour figure online)



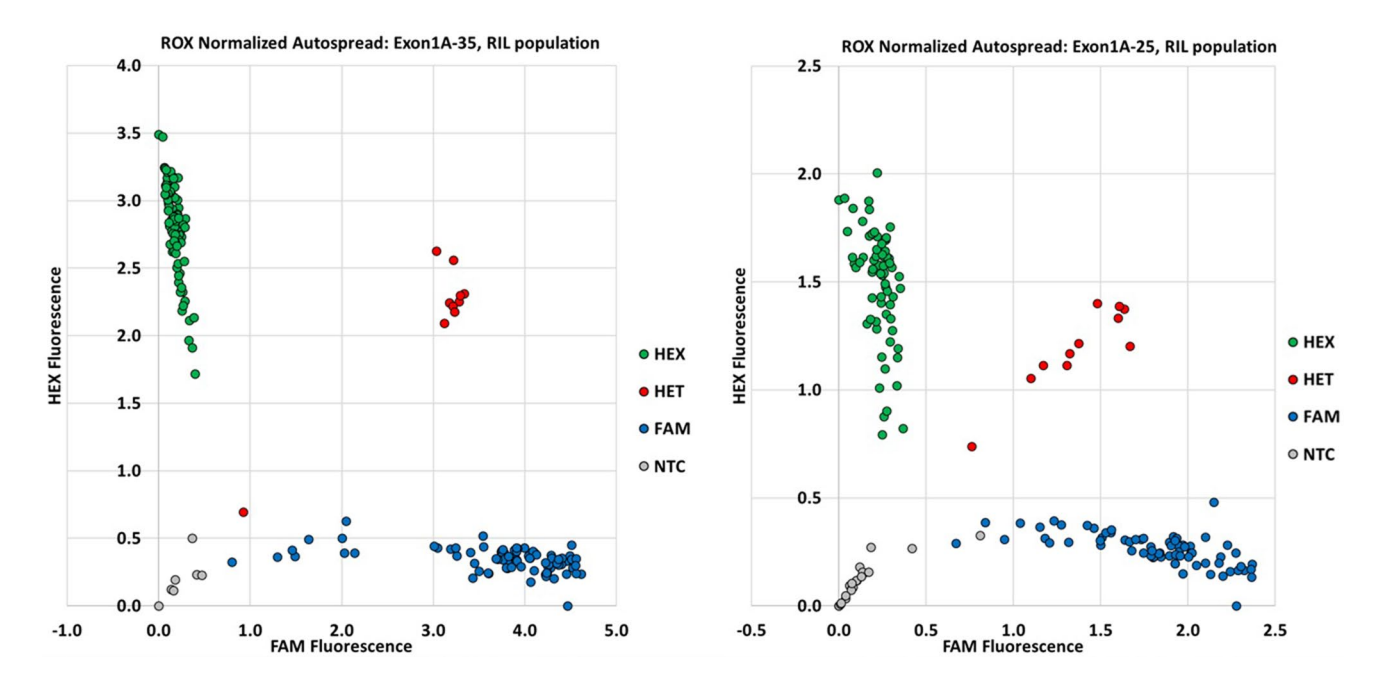


Fig. 3 KASP markers segregated in the recombinant inbred lines of JagMut1095×Jagger. The *X*- and *Y-axes* indicate the FAM and HEX fluorescence, respectively. The green and blue dots represent two

parental alleles of each marker, the red dots represent heterozygous genotypes, and the gray dots represent non-template controls (colour figure online)

under moderate and high-water stress treatments, and the drought tolerant cultivars maintained a higher osmotic adjustment (OA). As drought tolerance is a complicated trait and can be generated by different mechanisms such as cellular OA, water use efficiency (WUE), or morphological changes to reduce plant dehydration (Blum 2005; Cao et al. 2007), breeding for drought tolerance may need to consider multiple mechanisms together including RL.

In this study, a significantly positive correlation (r=0.40) was observed between RL and HD across the environments. As plants with a longer HD may have higher chance to catch drought and heat stresses in grain filling stage in the field, the significant positive correlation between RL and HD suggests the phenology changes can affect environments for plant growth and development. In the present study, a QTL for HD was detected on 1A in two environments and BLUE, and overlapped with QRl.hwwg-1AS. However, QRl.hwwg-1AS was significant in all the five environments, even at the seedling stage, thus, the two QTLs may be tightly linked. Further characterization of QRl.hwwg-1AS may shed a light on the RL mechanism and the interaction between plant phenology and responses to environmental changes.

Conclusion

In this study, we analyzed the RL trait in a wheat RILs and found two major QTLs (*QRl.hwwg-1AS* and *QRl.hwwg-5AL*) mainly responsible for the RL phenotype in JagMut1095.

QRl.hwwg-5AL was mapped in a 50 Mb interval in this study and it is likely the same QTL reported previously. *QRl.hwwg-1AS* mapped to a 6.04 Mb physical interval on 1AS showed the large effect in all five experiments and is a novel QTL identified in this study. Further fine mapping of *QRl.hwwg-1AS* will facilitate map-based cloning and further understanding of mechanisms of wheat drought tolerance.

Supplementary Information The online version contains supplementary material available at https://doi.org/10.1007/s00122-023-04284-3.

Acknowledgements This is contribution number 23-030-J from the Kansas Agricultural Experiment Station. Author thanks Dr. Michael Pumphrey for providing the Jagger mutant population. Mention of trade names or commercial products in this publication is solely for the purpose of providing specific information and does not imply recommendation or endorsement by the US Department of Agriculture. The USDA is an equal opportunity provider and employer.

Author contribution statement GB designed the research; RB, YX, SAP, and AB performed the research. NL and ZS conducted mutant screening. EA and KJ provided exome-capture data. RB, GZ, AF, and JR performed field phenotyping. RB and GB wrote the manuscript. All the authors provided inputs and approved the manuscript.

Funding Funding is provided by the US Wheat and Barley Scab Initiative, the Agriculture and Food Research Initiative Competitive Grant 2022-68013-36439 (WheatCAP) from the USDA National Institute of Food and Agriculture, and Chinese Scholarship Council.

Data availability All the data are included in the manuscript and the supplementary information.



Declarations

Conflict of interest The authors declare that they have no conflict of interest.

Ethical standards The authors declare that the experiments comply with the current laws of the country in which they were performed.

References

- Bai G, Kolb FL, Shaner G, Domier LL (1999) Amplified fragment length polymorphism markers linked to a major quantitative trait locus controlling scab resistance in wheat. Phytopathology 89:343–348. https://doi.org/10.1094/PHYTO.1999.89.4.343
- Baker NR, Rosenqvist E (2004) Applications of chlorophyll fluorescence can improve crop production strategies: an examination of future possibilities. J Exp Bot 55:1607–1621. https://doi.org/10.1093/jxb/erh196
- Blum A (2005) Drought resistance, water-use efficiency, and yield potential—Are they compatible, dissonant, or mutually exclusive? Aust J Agric Res 56:1159–1168. https://doi.org/10.1071/AR05069
- Bogard M, Hourcade D, Piquemal B et al (2021) Marker-based crop model-assisted ideotype design to improve avoidance of abiotic stress in bread wheat. J Exp Bot 72:1085–1103. https://doi.org/ 10.1093/jxb/eraa477
- Bradbury PJ, Zhang Z, Kroon DE et al (2007) TASSEL: software for association mapping of complex traits in diverse samples. Bioinformatics 23:2633–2635. https://doi.org/10.1093/bioinforma tics/btm308
- Cao HX, Zhang ZB, Xu P et al (2007) Mutual physiological genetic mechanism of plant high water use efficiency and nutrition use efficiency. Colloids Surf B 57:1–7. https://doi.org/10.1016/j.colsu rfb.2006.11.036
- Clarke JM (1986) Effect of leaf rolling on leaf water loss in Trilicam spp. J Plant Sci 66:8–13
- Corlett JE, Jones HG, Massacci A et al (1994) Water deficit, leaf rolling and susceptibility to photoinhibition in field grown sorghum. Physiol Plant 92:423–430. https://doi.org/10.1111/J.1399-3054. 1994.tb08831.x
- Doerge RW, Churchill GA (1996) Permutation tests for multiple loci affecting a quantitative character. Genetics 142:285–294. https:// doi.org/10.1093/genetics/142.1.285
- Fang L, Zhao F, Cong Y et al (2012) Rolling-leaf14 is a 2OG-Fe (II) oxygenase family protein that modulates rice leaf rolling by affecting secondary cell wall formation in leaves. Plant Biotech J 10:524–532. https://doi.org/10.1111/J.1467-7652.2012.00679.x
- Gao L, Yang G, Li Y et al (2019) Fine mapping and candidate gene analysis of a QTL associated with leaf rolling index on chromosome 4 of maize (*Zea mays* L.). Theor Appl Genet 132:3047–3062. https://doi.org/10.1007/S00122-019-03405-1
- Gouache D, le Bris X, Bogard M et al (2012) Evaluating agronomic adaptation options to increasing heat stress under climate change during wheat grain filling in France. Eur J Agron 39:62–70. https://doi.org/10.1016/J.EJA.2012.01.009
- Gupta PK, Balyan HS, Gahlaut V (2017) QTL analysis for drought tolerance in wheat: present status and future possibilities. Agronomy 7(1):5. https://doi.org/10.3390/agronomy7010005
- Hsiao TC, O'Toole JC, Yambao EB et al (1984) Influence of osmotic adjustment on leaf rolling and tissue death in rice (*Oryza sativa* L.). Plant Physiol 75:338–341. https://doi.org/10.1104/PP.75.2. 338
- Hu J, Zhu L, Zeng D et al (2010) Identification and characterization of NARROW AND ROLLED LEAF 1, a novel gene regulating

- leaf morphology and plant architecture in rice. Plant Mol Biol 73:283–292. https://doi.org/10.1007/S11103-010-9614-7
- International Wheat Genomic Sequencing Consortium (IWGSC) (2018) Shifting the limits in wheat research and breeding using a fully annotated reference genome. Science 361:eaar7191. https://doi.org/10.1126/science.aar7191
- Jordan K, Wang S, Lun Y et al (2015) A haplotype map of allohexaploid wheat reveals distinct patterns of selection on homoeologous genomes. Genome Biol 16(1):1–18. https://doi.org/10.1186/ S13059-015-0606-4
- Juarez MT, Kui JS, Thomas J et al (2004) microRNA-mediated repression of rolled leaf1 specifies maize leaf polarity. Nature 428:84–88. https://doi.org/10.1038/nature02363
- Kadioglu A, Terzi R (2007) A dehydration avoidance mechanism: leaf rolling. Bot Rev 73:290–302. https://doi.org/10.1663/0006-8101(2007)73[290:adamlr]2.0.CO;2
- Kim D, Langmead B, Salzberg SL (2015) HISAT: a fast spliced aligner with low memory requirements. Nat Methods 12:357-360
- Kosambi DD (1943) The estimation of map distances from recombination values. Ann Eug 12:172–175. https://doi.org/10.1111/j. 1469-1809.1943.tb02321.x
- Li H, Handsaker B, Wysoker A et al (2009) The sequence alignment/ map format and SAMtools. Bioinformatics 25:2078–2079. https:// doi.org/10.1093/Bioinformatics/btp352
- Liu X, Li M, Liu K et al (2016) Semi-rolled leaf2 modulates rice leaf rolling by regulating abaxial side cell differentiation. J Exp Bot 67:2139–2150. https://doi.org/10.1093/jxb/erw029
- McKenna A, Hanna M, Banks E et al (2010) The genome analysis toolkit: a mapreduce framework for analyzing next-generation DNA sequencing data. Genome Res 20:1297–1303. https://doi.org/10.1101/gr.107524.110
- Meng L, Li H, Zhang L et al (2015) QTL IciMapping: integrated software for genetic linkage map construction and quantitative trait locus mapping in biparental populations. Crop J 3:269–283. https://doi.org/10.1016/j.cj.2015.01.001
- Mysków B, Góralska M, Lenarczyk N et al (2018) Putative candidate genes responsible for leaf rolling in rye (*Secale cereale* L.). BMC Genet 19:1–11. https://doi.org/10.1186/S12863-018-0665-0/
- Obsa BT, Eglinton J, Coventry S et al (2016) Genetic analysis of developmental and adaptive traits in three doubled haploid populations of barley (*Hordeum vulgare* L.). Theor Appl Genet 129:1139–1151. https://doi.org/10.1007/S00122-016-2689-z
- Oppenheimer HR (1960). Adaptation to drought: xerophytism. Plantwater relationships in arid and semi-arid conditions: reviews of research. The United Nations Educulionul, Scientijc and Cultural Orgunizulion, Printed by C. J. Bucher, Lucerne, Swilzerland
- Patel RK, Jain M (2012) NGS QC Toolkit: a toolkit for quality control of next generation sequencing data. PLoS ONE 7:e30619. https://doi.org/10.1371/journal.0030619
- Peleg Z, Fahima T, Krugman T et al (2009) Genomic dissection of drought resistance in durum wheat × wild emmer wheat recombinant inbred line population. Plant Cell Environ 32:758–779. https://doi.org/10.1111/J.1365-3040.2009.01956.x
- Poland JA, Rife TW (2012) Genotyping-by-sequencing for plant breeding and genetics. Plant Genome 5:92. https://doi.org/10.3835/plant genome2012.05.0005
- Price AH, Young EM, Tomos AD (1997) Quantitative trait loci associated with stomatal conductance, leaf rolling and heading date mapped in upland rice (*Oryza sativa*). New Phytol 137:83–91. https://doi.org/10.1046/J.1469-8137.1997.00818.x
- Qiang Z, Tianqing Z, Long H et al (2016) Joint mapping and allele mining of the rolled leaf trait in rice (*Oryza sativa* L.). PLoS ONE 11:e0158246. https://doi.org/10.1371/JOURNAL.PONE.0158246
- Rawat N, Joshi A, Pumphrey M et al (2019) A tilling resource for hard red winter wheat variety Jagger. Crop Sci 59:1666–1671. https:// doi.org/10.2135/CROPSCI2019.01.0011



- Saglam A, Kadioglu A, Demiralay M et al (2014) Leaf rolling reduces photosynthetic loss in maize under severe drought. ACTA Bot Croat 73:315–323. https://doi.org/10.2478/botcro-2014-0012
- Saneoka H, Ogata S, Agata W (1996) Cultivar differences in dry matter production and leaf water relations in water-stressed maize (*Zea mays* L.). Jpn J Grassl Sci 41(4):294–301
- Shiferaw B, Smale M, Braun HJ et al (2013) Crops that feed the world 10. past successes and future challenges to the role played by wheat in global food security. Food Sec 5:291–317. https://doi.org/10.1007/s12571-013-0263-y
- Singh BN, Mackill DJ (2008) Genetics of leaf rolling under drought stress. Rice Genet II:159–166. https://doi.org/10.1142/97898 12814272 0015
- Singh S, Singh TN (2000) Significance of leaf rolling in rice during water stress. Ind J Plant Physiol 5:214–218
- Sommer R, Glazirina M, Yuldashev T et al (2013) Impact of climate change on wheat productivity in Central Asia. Agric Ecosyst Environ 178:78–99. https://doi.org/10.1016/j.agee.2013.06.011
- Tahmasebi S, Heidari B, Pakniyat H et al (2016) Mapping QTLs associated with agronomic and physiological traits under terminal drought and heat stress conditions in wheat (*Triticum aestivum* L.). Genome 60:26–45. https://doi.org/10.1139/gen-2016-0017
- Timmermans MCP, Schultes NP, Jankovsky JP et al (1998) Leafbladeless1 is required for dorsoventrality of lateral organs in maize. Development 125:2813–2823. https://doi.org/10.1242/dev.125.15.2813
- Turgut R, Kadioglu A (1998) The effect of drought, temperature and irradiation on leaf rolling in Ctenanthe setosa. Biol Plant 41:629–633, https://doi.org/10.1023/A:1001817105685
- Turner NC, Begg JE (1981) Plant-water relations and adaptation to stress. Plant Soil 58:97–131. https://doi.org/10.1007/bf02180051
- Untergasser A, Cutcutache I, Koressaar T et al (2012) Primer3-new capabilities and interfaces. Nucleic Acids Res 40:e115. https://doi.org/10.1093/nar/gks596

- Verma A, Niranjana M, Jha SK et al (2020) QTL detection and putative candidate gene prediction for leaf rolling under moisture stress condition in wheat. Sci Rep 10:1–13. https://doi.org/10.1038/s41598-020-75703-4
- Wang JK (2009) Inclusive composite interval mapping of quantitative trait genes. Acta Agron Sin 35:239–245. https://doi.org/10.3724/sp.j.1006.2009.0023
- Wang S (2007) Windows QTL cartographer 2.5
- Xiang JJ, Zhang GH, Qian Q et al (2012) Semi-Rolled Leaf1 encodes a putative glycosylphosphatidylinositol-anchored protein and modulates rice leaf rolling by regulating the formation of bulliform cells. Plant Physiol 159:1488–1500. https://doi.org/10.1104/pp. 112.199968
- Xu Y, Wang Y, Long Q et al (2014) Overexpression of OsZHD1, a zinc finger homeodomain class homeobox transcription factor, induces abaxially curled and drooping leaf in rice. Planta 239:803–816. https://doi.org/10.1007/S00425-013-2009-7
- Xu P, Ali A, Han B et al (2018) Current advances in molecular basis and mechanisms regulating leaf morphology in rice. Front Plant Sci. https://doi.org/10.3389/FPLS.2018.01528
- Zou LP, Sun XH, Zhang ZG et al (2011) Leaf rolling controlled by the homeodomain leucine zipper class IV gene Roc5 in rice. Plant Physiol 156:1589–1602. https://doi.org/10.1104/PP.111.176016

Publisher's Note Springer Nature remains neutral with regard to jurisdictional claims in published maps and institutional affiliations.

